BIOCHEMISTRY
including biophysical chemistry & molecular biology

ARTICLE

pubs.acs.org/biochemistry

Rate-Limiting Domain and Loop Motions in Arginine Kinase

Omar Davulcu,[†] Jack J. Skalicky,[‡] and Michael S. Chapman*[,†]

[†]Department of Biochemistry and Molecular Biology, Oregon Health and Science University, Portland, Oregon 97239-3098, United States

[‡]Department of Biochemistry, University of Utah, Salt Lake City, Utah 84112-5650, United States

Supporting Information

ABSTRACT: Arginine kinase catalyzes the reversible transfer of a phosphoryl group between ATP and arginine. It is the arthropod homologue of creatine kinase, buffering cellular ATP levels. Crystal structures of arginine kinase, in substrate-free and substrate-bound forms, have revealed large conformational changes associated with the catalytic cycle. Recent nuclear magnetic resonance identified movements of the N-terminal domain and a loop comprising residues I182−G209 with conformational exchange rates in the substrate-free enzyme similar to the turnover rate. Here, to understand whether these motions might be rate-limiting, we determined activation barriers for both the intrinsic dynamics and enzyme turnover using measurements over a temperature range of 15−30 °C. ^{15}N transverse relaxation dispersion yields activation barriers of 46 ± 8 and 34 ± 12 kJ/mol for the N-terminal domain and I182−G209 loop, respectively. An activation barrier of 34 ± 13 kJ/mol was obtained for enzyme turnover from steady-state kinetics. The similarity between the activation barriers is indeed consistent with turnover being limited by backbone conformational dynamics and pinpoints the locations of potentially rate-limiting motions.

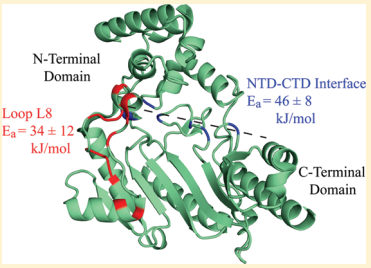

Arginine kinase (EC 2.7.3.3) is a member of the phosphagen kinase family of enzymes and catalyzes the reversible transfer of a phosphoryl group between ATP and arginine. Found primarily in invertebrates, arginine kinase acts to buffer cellular levels of ATP in cells with high or variable demands for energy.[1] In addition to its important physiological role, the phosphagen kinase family has been the focus of much research aimed at understanding bimolecular enzyme catalysis.[1] Arginine kinase from the Atlantic horseshoe crab *Limulus polyphemus*, a 42 kDa monomer, is selected as a model system for investigating the link between enzyme dynamics and function, in part because of its amenability to both high-resolution X-ray crystallography and nuclear magnetic resonance (NMR) spectroscopy.[2−6]

Steady-state enzyme kinetics have revealed the arginine kinase kinetic mechanism to be a rapid equilibrium, random-order bimolecular−bimolecular reaction, with a turnover number (k_{cat}) of approximately 135 s^{-1} at 25 °C.[7−9] The enzyme has also been shown to undergo large conformational changes during the catalytic cycle. Initially, X-ray solution scattering experiments revealed a decrease in the radius of gyration of the enzyme associated with substrate binding.[10] The locations and degree of these protein conformational changes were not evident, however, until X-ray crystal structures of the enzyme became available.

Two crystal structures of *L. polyphemus* arginine kinase highlight the conformational changes associated with substrate binding. The first, in a substrate-free or "open" state, was initially determined at 2.4 Å resolution and recently extended to 1.7 Å.[4,11] The second structure, with a transition-state analogue bound to form a "closed" state, was determined at 1.2 Å resolution and contained enzyme-bound MgATP, arginine, and nitrate, with the latter mimicking the phosphoryl group being transferred.[5,6] Overall, these structures established arginine kinase as a two-domain enzyme, with a primarily α-helical N-terminal domain (NTD) spanning residues 1−90 and a primarily β-sheet C-terminal domain (CTD) spanning residues 120−357. These two domains are joined via a 29-residue flexible linker. Comparison of these crystal structures shows a closing of the NTD and CTD along with folding of a set of loops over the active site (Figure 1). In general terms, the substrate-associated conformational changes have been described as a hand making a grabbing motion.[4−6,11] A similar set of conformational changes has been observed in creatine kinase, an arginine kinase homologue.[12−14]

The open and closed crystal structures of arginine kinase provide "snapshots" of the enzyme during the catalytic cycle. They give insight into the amplitudes of conformational changes but not the associated rates. Recently, NMR-based ^{15}N spin relaxation experiments with substrate-free arginine kinase have highlighted the backbone dynamics intrinsic to the enzyme on a wide range of time scales.[3] Lipari−Szabo analysis pinpointed loop L13, residues V308−V322, with intrinsic dynamics on the nanosecond time scale.[15,16] ^{15}N transverse relaxation dispersion experiments indicated that approximately 12% of the protein was involved in micro- to millisecond time scale dynamics in the absence of substrate.[17−19] Residues exhibiting these slow dynamics localized to four regions in the enzyme: (1) the interface and (2) hinge between the NTD and CTD; (3) loop L8,

Received: October 15, 2010
Revised: March 18, 2011
Published: March 22, 2011

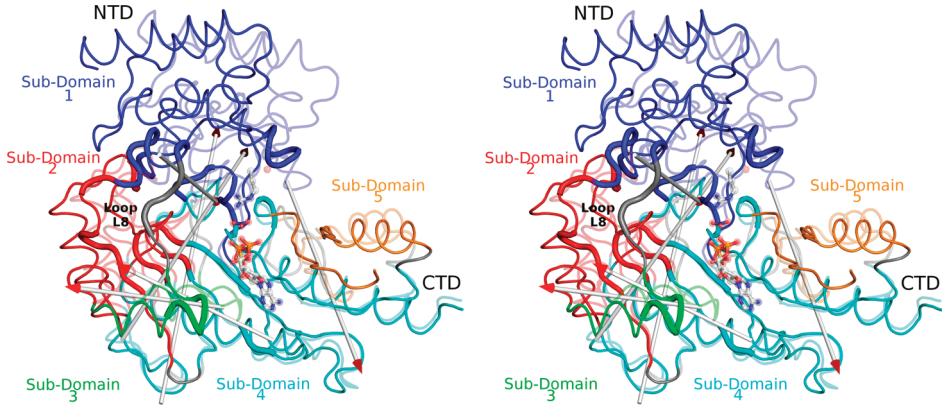

Figure 1. Conformational changes associated with substrate binding in arginine kinase. The stereopair shows the substrate-free (opaque) and transition-state analogue (transparent) crystal structures of arginine kinase. Subdomains 1−5 are colored blue, red, green, cyan, and orange, respectively; flexible residues that are not a member of any quasi-rigid subdomain are colored gray. Axes of rotation between subdomains are shown with arrows. Residues previously shown by NMR relaxation dispersion experiments to be undergoing micro- to millisecond time scale dynamics are shown with thicker traces.[3]

spanning residues I182−G209; and (4) several segments of the primary structure that together form the center of the CTD β-sheet (Figure 1). Interestingly, the rates of motion for the NTD and loop L8 were commensurate with the turnover rate, suggesting that one or both of these conformational changes might be rate-limiting upon turnover.[3]

The importance of protein motions for enzyme function has long been hypothesized; furthermore, there has been long-standing speculation that protein conformational changes could be rate-limiting for some.[20] It is only recently, however, that experimental techniques have been developed to probe conformational changes. Recent advances in NMR have allowed for the direct measurement of rates of protein motions at the residue level.[21] This technique has allowed for determination of protein motions critical for turnover in systems such as triosephosphate isomerase, cyclophillin A, RNase A, and dihydrofolate reductase.[21−24]

The work presented here builds upon the previous work exploring the intrinsic dynamics of arginine kinase.[3] To further test the hypothesis that protein conformational changes are rate-limiting on turnover, we perform ^{15}N transverse relaxation dispersion experiments along with enzyme kinetic measurements across a temperature range of 15−30 °C.[17−19] Conformational exchange rates (k_{ex}) and turnover rates (k_{cat}) are obtained as a function of temperature, thus allowing access to activation energies associated with intrinsic conformational changes and the entire catalytic cycle, respectively. The activation barriers of the NTD and loop L8 motions were found to be similar to that of the catalyzed reaction, thus providing further evidence that one or both of these conformational changes are rate-limiting upon arginine kinase turnover.

MATERIALS AND METHODS

Sample Preparation. *L. polyphemus* arginine kinase uniformly ^{15}N-enriched and ∼80% ^{2}H-enriched was expressed and purified as previously described, using urea-based unfolding and refolding to allow for exchange of amide deuterons with protons in the core of the enzyme.[2,9] Enzyme to be used for NMR was concentrated to 1 mM (42 mg/mL) in a buffer containing 10 mM sodium citrate (pH 6.5), 0.5 mM dithiothreitol, 50 mM potassium chloride, 50 μM sodium azide, and 10% $^{2}H_2O$. Enzyme for use in kinetic assays was stored at 2 mg/mL in 10 mM Tris (pH 8.0), 1 mM dithiothreitol, and 100 mM potassium chloride. Protein concentrations were measured spectrophotometrically with an extinction coefficient of 0.76 mL mg^{-1} cm^{-1} at 280 nm.

Collection and Analysis of NMR Data. NMR data were collected on Varian INOVA spectrometers operating at a ^{1}H (^{15}N) Larmor frequency of 599.7 (60.78), 719.9 (72.95), or 799.7 (81.04) MHz. Each spectrometer was equipped with a HCN triple-resonance probe and *Z*-axis pulsed field gradient. Relaxation experiments were performed at 15, 20, 25, and 30 °C with temperature calibration achieved using a methanol standard.[25] ^{1}H chemical shifts were referenced to the methyl protons of DSS at 0 ppm; ^{15}N chemical shifts were referenced indirectly.[26] ^{1}H and ^{15}N backbone amide resonance assignments have previously been reported.[2]

Chemical exchange on the micro- to millisecond time scale was quantified using a constant-time ^{15}N spin CPMG relaxation dispersion approach with TROSY detection.[18] These experiments were performed at the three static fields listed above. The CPMG effective field strength (υ) ranged from 0 to 1 kHz via modulation of the refocusing delay time. Individual relaxation dispersion data sets were collected with the following parameters: ^{15}N ω_0 = 60.78 MHz, constant relaxation time of 40 ms, υ = 0, 25, 50*, 100, 200, 250, 300, 400, 500, 625, 750, 875, and 1000 Hz; ^{15}N ω_0 = 72.95 and 81.04 MHz, constant relaxation time of 32 ms, υ = 0*, 31.25, 62.50, 93.75, 125*, 156.25, 187.50, 250, 375, 500*, 625*, 750, 875, and 1000* Hz. Asterisks denote points that were measured in duplicate and used in error estimation. Data sets at all three static fields were collected at 15 and 25 °C; data sets at ^{15}N ω_0 = 81.04 MHz were also collected at 20 and 30 °C. All relaxation data were recorded with a ^{1}H acquisition time of ∼100 ms and a ^{15}N acquisition time of 75 ms (t_{1max}) and were processed with FELIX2004 (Accelrys, Inc.) to a final matrix dimension of 4096 (^{1}H) × 1024 (^{15}N) points.

^{15}N R_2^{eff} was determined at each CPMG field strength by a two-point logarithmic function: $R_2^{eff} = (-1/\tau_{relax}) \ln(I_\upsilon/I_0)$. In this relationship, τ_{relax} is the constant-time relaxation period, I_υ is the intensity of any given resonance at CPMG effective field strength υ, and I_0 is the intensity of the resonance in the reference experiment omitting the CPMG block. Measured ^{15}N R_2^{eff} values are listed in Table 1 of the Supporting Information. Subsequently,

the Bloch−McConnell or Carver−Richards equations were fit to the resulting R_2^{eff} values at all four temperatures simultaneously with software provided by L. Kay and D. Korzhnev.[17] This fitting, in all cases, assumed two-state exchange, yielding, for each temperature, an exchange rate constant k_{ex}, which is the sum of the forward and reverse rate constants. For some groups of residues, it was also possible to estimate the relative populations of states A (p_A) and B (p_B) and the ^{15}N chemical shift difference between states A and B ($\Delta\omega$). Errors in each of these parameters were obtained from the least-squares fitting. No assumption was made with regard to the fast or slow exchange regime of k_{ex} relative to $\Delta\omega$. Measured R_2^{eff} values at all static field strengths for those residues showing chemical exchange at 15, 20, 25, and 30 °C are listed in Table 2 of the Supporting Information.

With R_{ex} determined at multiple static fields, the time scale of chemical exchange can be determined from calculation of a parameter previously described as α.[27] Note that this is distinct from the synergy constant, also α by convention, associated with determination of k_{cat} (see below). In the context of NMR chemical exchange, α is defined as

$$\alpha = \frac{B_{02} + B_{01}}{B_{02} - B_{01}} \times \frac{R_{ex2} - R_{ex1}}{R_{ex2} + R_{ex1}}$$

where, for any given residue, B_{01} and B_{02} are the static magnetic field strengths of the lower and higher fields, respectively, and R_{ex1} and R_{ex2} are the chemical exchange contributions to R_2^{eff} determined at two field strengths. Errors in α were calculated by propagation of the errors in R_{ex1} and R_{ex2}. Ideally, α adopts values between 0 and 2, differentiating between slow exchange ($\alpha < 1$), intermediate exchange ($\alpha \sim 1$), and fast exchange ($\alpha > 1$). k_{ex} is typically well-determined regardless of the exchange time scale; however, for residues in fast exchange, the only other well-determined parameter is the $p_A p_B \Delta\omega$ product.[27,28] Individual p_A, p_B, and $\Delta\omega$ values can be determined, on the other hand, for residues in slow to intermediate exchange. Furthermore, in the slow to intermediate exchange regime, k_{ex} can be decomposed into k_{slow} and k_{fast}, where $k_{slow} = k_{ex}p_B$, $k_{fast} = k_{ex}p_A$, and $k_{ex} = k_{slow} + k_{fast}$.

To obtain activation barriers of intrinsic dynamics measured by NMR, we performed nonlinear least-squares fitting of the Arrhenius equation to the temperature-dependent values of both k_{slow} and k_{ex} in SigmaPlot (SPSS, Inc.). Errors in the activation barriers came from least-squares fitting.

Enzyme Kinetics and Data Analysis. Arginine kinase activity was measured using a coupled enzyme assay in the forward direction (synthesis of phosphoarginine) following standard procedures.[29,30] This assay couples production of ADP by arginine kinase to dephosphorylation of phosphoenolpyruvate by pyruvate kinase and reduction of pyruvate by NADH-dependent lactate dehydrogenase. The conversion of NADH to NAD^+ is measured through absorbance at 340 nm. Measurements were performed on a Varian Cary 100 UV−vis spectrophotometer capable of monitoring six samples simultaneously.

The final reaction mixture included 100 mM Tris-acetate (pH 8), 6 mM magnesium acetate, 133 mM potassium chloride, 1.2 mM phosphoenolpyruvate, 0.5 mM NADH, and 6.5 EU each of pyruvate kinase and lactate dehydrogenase. Nominal ATP concentrations were 0.08, 0.16, 0.32, 0.64, 0.96, and 1.4 mM; nominal arginine concentrations were 0.2, 0.4, 0.8, 1.6, 3.2, and 7.0 mM. Thus, for each assay, 36 individual velocity measurements were obtained. ATP stock concentrations were standardized by measuring the absorbance at 260 nm with an extinction coefficient of 15.4 mM^{-1} cm^{-1}. Arginine stock concentrations were standardized spectrophotometrically with the enzymatic assay and ATP in excess.

Reaction mixtures were allowed to incubate for 10 min to reach the desired temperature. The reaction was then initiated by addition of arginine kinase to the mixture and was allowed to proceed for 5 min. Initial velocities were obtained from the average slope of the linear range of the absorbance profile for each reaction. Each full assay was measured in triplicate and at nominal temperatures of 15, 20, 25, and 30 °C, for a total of 12 measurements. Actual temperatures were measured at six points during each full assay. The largest intra-assay temperature variance was 0.5 °C. For each assay, the average of these six temperature measurements was used in data analysis.

Initial velocities obtained from each assay were fit to the rate equation for a rapid equilibrium, random-order, bimolecular−bimolecular reaction:[31,32]

$$v = \frac{V_{max}[Arg][ATP]}{\alpha K_{S(Arg)}K_{S(ATP)} + \alpha K_{S(Arg)}[ATP] + \alpha K_{S(ATP)}[Arg] + [Arg][ATP]}$$

where K_S is the dissociation constant for a given enzyme−substrate complex and $\alpha = K_m/K_S$. V_{max} was fitted by nonlinear least-squares regression in SigmaPlot (SPSS, Inc.) to the 36 velocity measurements for each assay and then converted to k_{cat}. Error estimates come from the least-squares fitting.

Activation barriers for the enzyme-catalyzed reaction were determined by fitting the Arrhenius equation to k_{cat} determined at the four temperatures (see above), again using nonlinear least-squares regression in SigmaPlot (SPSS, Inc.). Errors in the activation barrier of the catalyzed reaction came from least-squares fitting.

RESULTS

Slow, Micro- to Millisecond Time Scale Intrinsic Dynamics. Summed rate constants ($k_{ex} = k_{forward} + k_{reverse}$) of intrinsic, backbone motions in arginine kinase were fitted using ^{15}N transverse relaxation dispersion data with the Carver−Richards or Bloch−McConnell equations and assuming a two-state exchange model. This approach provides a direct measure of exchange kinetics, resulting from ^{15}N nuclei alternating between different magnetic environments, or chemical states.[17,18,21] The activation barrier for exchange can be measured from the temperature dependence of the rate constant k_{ex}.[33] Dynamics intrinsic to substrate-free arginine kinase at 25 °C have been previously described;[3] here, similar experiments were conducted at three additional temperatures, thus allowing the determination of the activation energies.

Overlaid ^{15}N−^{1}H TROSY spectra of arginine kinase recorded at 15, 20, 25, and 30 °C are shown in Figure 2. Peak positions vary within the range of typical H^N thermal coefficients,[34] and full enzyme activity is retained (see below), indications that the protein is stable and not unfolding over the temperature range. Representative ^{15}N transverse relaxation dispersion profiles for two residues undergoing chemical exchange are shown in Figure 2. The numbers of amino acid residues with R_{ex} values of >2 s^{-1} at 15, 20, 25, and 30 °C are 33, 23, 34, and 28, respectively, and are further analyzed below. As previously observed, residues with R_{ex} predominantly localize to four spatial regions of the enzyme: the hinge between the NTD and CTD, the interface between the NTD and CTD, the core β-sheet at the

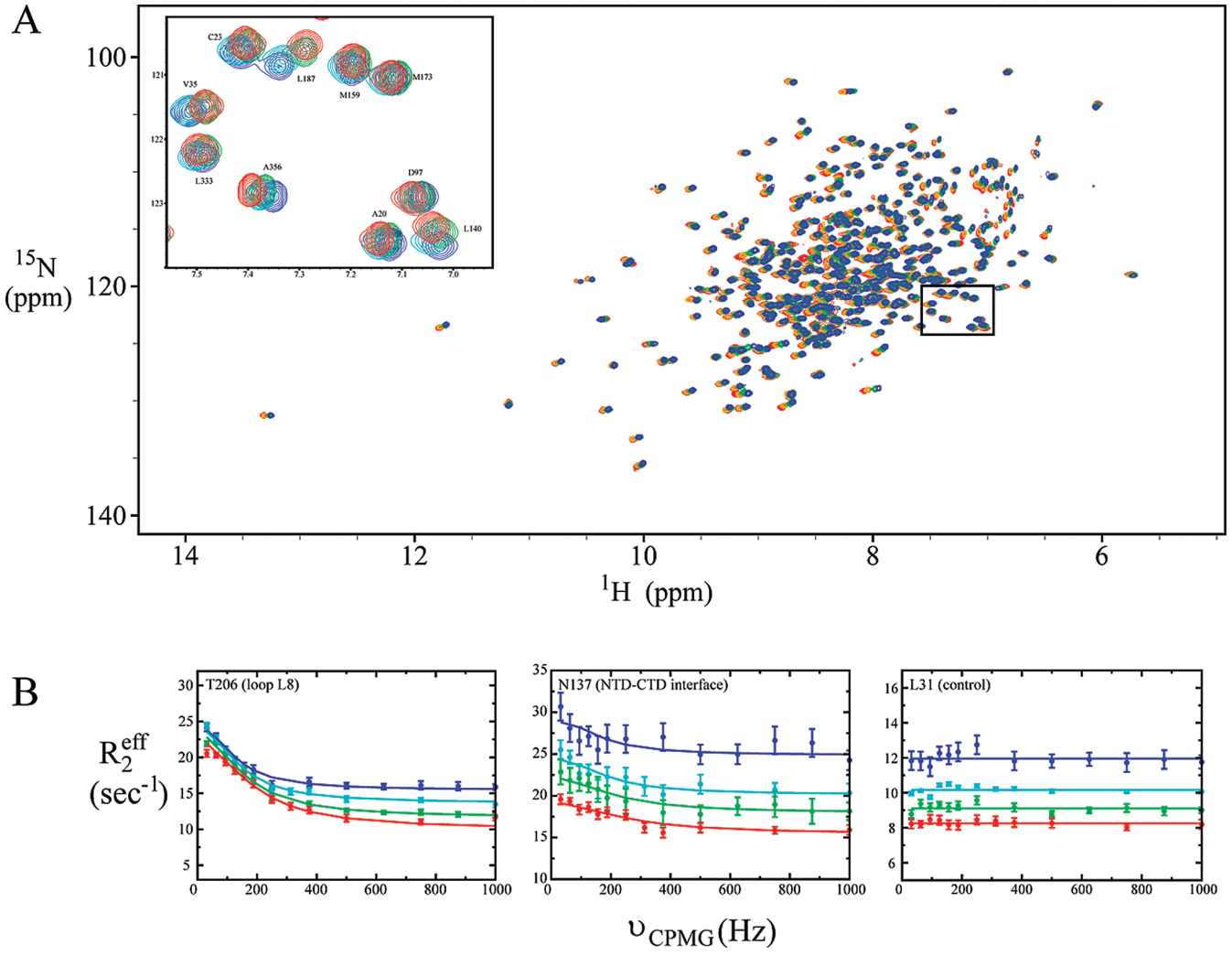

Figure 2. (A) Two-dimensional ^{15}N−^{1}H TROSY spectra of arginine kinase recorded at 800 MHz and 15 (blue), 20 (cyan), 25 (green), and 30 °C.[28] The boxed region is expanded in the inset. (B) Collectively fit ^{15}N transverse relaxation dispersion curves for T206 (left) and N137 (right), representative of loop L8 and the NTD−CTD interface, respectively. L31, a motionless control, is also shown. Data shown were collected at a ^{15}N Larmor frequency of 81.04 MHz at 15 (blue), 20 (cyan), 25 (green), and 30 °C.[28] Errors are estimated from duplicate measurements of R_2^{eff}.

active site, and the substrate binding loop spanning residues I182−G209.[3] In the prior single-temperature analysis, it had been shown that unified chemical exchange parameters (single k_{ex} and p_B values determined collectively for sets of residues), appropriate for concerted group motion of each of the four regions, yielded an excellent fit, and the same proved to be true here. Robust fitting of activation barriers is possible for two of these four regions: loop L8 and the NTD−CTD interface.

The level to which R_{ex} can be interpreted, individual rate constants and state populations, or merely exchange rates, depends on the exchange regime, parametrized by α. α values, determined from the static field dependence of R_{ex}, are listed in Table 3 of the Supporting Information for residues undergoing chemical exchange and indicate the residue's exchange regime [fast, intermediate, or slow (see Materials and Methods)]. In the NTD−CTD interface, α is ill-defined, due, in part, to high fractional errors in the small values of R_{ex}. Without evidence that exchange is in the slow or intermediate regime at the interface, analysis is limited to k_{ex}, which cannot be decomposed into k_{slow} and k_{fast}. For loop L8, errors in α similarly preclude designation of the exchange regime for many residues, but the three residues with well-determined α values all indicate an intermediate regime, even where α is expected to be highest at 25 °C: E190 with an α of 1.15 ± 0.22, D192 with an α of 1.33 ± 0.34, and T206 with an α of 1.12 ± 0.21. Thus, it is possible to fit p_A, p_B, and $\Delta\omega$ collectively to the relaxation dispersion profiles of the three residues with demonstrably slow intermediate exchange. The fitting of k_{ex} is not subject to the same exchange regime constraints, and the successful modeling of the entire loop with a single k_{ex} indicated concerted motion. Combining the loop L8 k_{ex} with the subsample p_B gives an approximate estimate of k_{slow} for a concerted two-state motion, albeit based on only three residues. At this point, the distinction between k_{slow} that, with the sparse data available, must be interpreted tentatively and conformational activation barriers derived from more robust k_{ex} values, which are fit to data from larger groups of residues without restrictions on exchange regimes, should be emphasized.

Should an enzyme's turnover be limited by conformational change, then one would expect correspondence of k_{cat} with k_{slow}, the slower of the conformational $k_{forward}$ or $k_{reverse}$. In cases where

Table 1. Chemical Exchange Parameters and Activation Barriers for Intrinsic Motions in Arginine Kinase[a]

cluster	temp (°C)	k_{ex} (s^{-1})	p_B (%)	k_{close} (s^{-1})	E_a (kJ/mol)
NTD−CTD interface	15	570 ± 120	–	–	46 ± 8
	20	790 ± 170			
	25	1070 ± 230			
	30	1440 ± 310			
loop L8	15	530 ± 80	3.5 ± 0.3	19 ± 3	34 ± 12
	20	680 ± 100	4.1 ± 0.5	28 ± 5	
	25	860 ± 120	4.9 ± 0.5	42 ± 7	
	30	1080 ± 150	5.7 ± 1.6	62 ± 19	

[a] p_B and k_{close} for the NTD−CTD interface are indeterminate because of the uncertainty in the chemical shift time scale. p_B for loop L8 is assumed to be the value obtained by collectively fitting residues in slow to intermediate exchange [E190, D192, and T206 (see Materials and Methods and Results)].

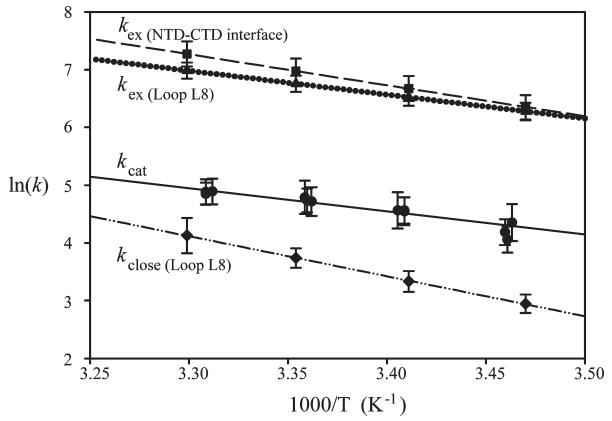

Figure 3. Arrhenius plots of k_{cat} (circles, solid line), collective k_{ex} for loop L8 (triangles, dotted line) and the NTD−CTD interface (squares, dashed line), and k_{close} for loop L8 (diamonds, dashed−dotted line). Errors are obtained from least-squares fitting (see Materials and Methods). The similarity of the slopes is indicative of similar activation barriers. Data shown here are for illustrative purposes; activation barriers were determined from least-squares fitting of the Arrhenius equation.

$k_{slow} \ll k_{fast}$ (where p_A and p_B are very different), k_{slow} can be regarded as the "rate-limiting step" of an exchange process described by k_{ex}. As such, the temperature dependence of k_{ex} is dominated by k_{slow}. Thus, k_{ex} can be used as a proxy for k_{slow} in analysis of activation barriers for turnover and conformational change. Use of k_{ex} circumvents the assumption of slow-to-intermediate exchange in calculating k_{slow} and experimental errors in measuring small values of p_B. Activation barriers calculated from k_{ex} could be regarded as an approximation of those calculated from k_{slow}. For loop L8, activation barriers can be calculated both ways (see below), and they agree within experimental error, giving confidence that either k_{ex} or k_{slow} can be the basis of comparison to k_{cat}.

Table 1 summarizes k_{ex} values obtained from fitting R_2^{eff} with the Bloch−McConnell or Carver−Richards equations. The activation energy barrier, E_a, associated with the dynamic processes derives from an Arrhenius analysis.[17] Residues in loop L8 and the NTD−CTD interface display a clear dependence of k_{ex} on temperature (Table 1). When residues of each cluster are fitted together, a similar range of k_{ex} values is observed between 15 and 30 °C: 500−1100 s^{-1} for loop L8 and 600−1400 s^{-1} for the NTD−CTD interface.

Within the temperature range described above, the fitted minor state populations, p_B, obtained from collective fitting of

Table 2. Temperature Dependence of the Turnover Number (k_{cat}) for Arginine Kinase Obtained from Steady-State Kinetics

temp (°C)	k_{cat} (s^{-1})	temp (°C)	k_{cat} (s^{-1})
15.9	66 ± 15	24.6	120 ± 35
15.6	78 ± 25	24.3	112 ± 28
15.8	58 ± 13	24.5	114 ± 23
20.5	96 ± 30	28.8	133 ± 30
20.2	94 ± 23	29.1	132 ± 28
20.2	96 ± 22	29.1	128 ± 24

E190, D192, and T206, are 3−6% for loop L8. The populations are correlated with temperature (Table 1) and likely reflect a real but modest temperature dependence of p_A and p_B.[35] However, caution is needed, because the temperature-based differences in p_B are barely larger than the estimated experimental error. Arrhenius plots derived from the k_{ex} and k_{close} exchange rates for loop L8 and the NTD−CTD interface are shown in Figure 3.

For loop L8, with the caveats already noted, k_{ex} can be decomposed into $k_{forward}$ and $k_{reverse}$ defined as $p_A k_{ex}$ and $p_B k_{ex}$, respectively. We assume that, in the absence of substrates, the majority population resembles the open form of the enzyme and the minority population lies along the path toward the closed form. Thus, $k_{forward}$ refers to the rate of closure ($k_{close} = p_B k_{ex}$). Conversely, $k_{reverse}$, the rate of opening of the minority population, is then $k_{open} = p_A k_{ex}$. Values of k_{close} are listed in Table 1 for loop L8.

Simultaneous, multitemperature fitting of k_{ex} for two clusters of residues, the NTD−CTD hinge and those lying in the core β-sheet, did not converge, precluding further analysis of these residues. This appears to be due to relatively large fractional errors in some of the smaller values of R_{ex}, leading to ill-conditioned fitting. This is not unexpected. Relaxation dispersion is a derivative measurement, a change in relaxation as a function of field. With temperature dependence, the dependent variable is a second derivative, small in value, and sensitive to errors especially if the temperature range is modest.

Enzyme-Catalyzed Reaction. Activation barriers for the reaction catalyzed by arginine kinase are determined by measurement of k_{cat} at varying temperatures. The same temperatures used for the NMR experiments described above, 15, 20, 25, and 30 °C, are used in the enzyme assay. Measured k_{cat} values are listed in Table 2. k_{cat} is observed to range from approximately 60 to 130 s^{-1}, with a clear dependence on temperature.

dx.doi.org/10.1021/bi101664u |*Biochemistry* 2011, 50, 4011–4018

The associated activation barrier for the enzyme-catalyzed reaction is 34 ± 4 kJ/mol. Figure 3 shows the Arrhenius plot obtained for arginine kinase.

At 25 °C, the k_{cat} values determined here are in agreement with previously published results.[8,9] This is in spite of kinetics being performed on a deuterated enzyme for the sake of compatibility with the NMR. k_{cat} was determined for the forward reaction (phosphoarginine production), but the values are consistent with previous measurements of the reverse reaction (ATP production) when phosphoarginine was available commercially. Furthermore, the kinetic parameters for the enzyme-catalyzed reaction determined here are also similar to those of orthologous enzymes.[36−38]

DISCUSSION

The conformational changes in arginine kinase associated with substrate binding have recently been described by rotations of five quasi-rigid groups.[39] These clusters of residues are sometimes noncontiguous in primary sequence, but their motion can be approximated by a common rotational and translational operation. Rotation of the five groups accounts for most of the differences between the open and closed forms of arginine kinase. Figure 1 maps these five quasi-rigid groups to the crystal structures of arginine kinase.

In addition to substrate-associated conformational changes, recent work has shown that arginine kinase is a highly dynamic enzyme in the absence of substrates.[3] Using NMR spectroscopy, this previous work highlighted the intrinsic loop and rigid-body domain motions of the enzyme on time scales ranging from picoseconds to milliseconds. Interestingly, the rates of intrinsic rotation of the N-terminal domain (NTD, residues 1−90) and motion of a substrate binding loop (loop L8, residues 182−201) were similar to k_{cat}, indicating that a protein conformational change might be rate-limiting. It has been hypothesized for quite some time that some conformational change, as opposed to the chemical step of phosphoryl transfer, might be rate-limiting on the arginine kinase reaction.[36] However, identification of specific candidate conformational change(s) is a recent development.[3]

Two of the previously described motions with turnover-commensurate rates are shown here to have activation barriers similar to that of the catalyzed reaction.[3] These are overall motion of the N-terminal domain, implied from exchange in the NTD−CTD interface region, and loop L8. X-ray crystal structures of the open and closed states of arginine kinase show that these regions also undergo changes associated with substrate binding.[4−6,11] Once the substrate bound, the NTD was shown to undergo a hinged, rigid-body rotation of ∼14° about residues 88−94. Loop L8 was shown to move more than 5 Å in a manner more complicated than a simple, rigid-body motion.[4−6] The motions of the NTD, loop L8, and other smaller movements bring catalytically important residues into the active site, likely align the substrates precisely for phosphoryl transfer, and shield reactive substrate atoms from water.[13,40−42] The rotation of the NTD brings the substrate specificity loop, residues L61−Y68, over the amino acid end of substrate arginine. Motion of loop L8 allows for formation of a hydrogen bond between the side chain of H185 and the ribose ring of the substrate nucleotide. Furthermore, an interaction between the NTD and loop L8 is also created in the closed state of the enzyme in the form of a salt bridge between residues R193 and D62.[4−6,11] It has been suggested that this interaction helps to stabilize the conformation

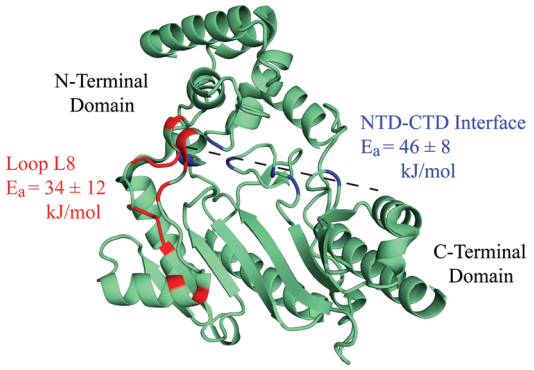

Figure 4. Rate-limiting conformational changes in arginine kinase. Shown is a ribbon diagram of the substrate-free crystal structure of arginine kinase, with N- and C-terminal domains labeled.[39] Residues exhibiting chemical exchange and used to determine activation barriers of intrinsic backbone dynamics lie in two regions of the enzyme: loop L8 (I182−G209, red) and the interface between the N- and C-terminal domains, denoted by a dotted line (blue). The activation barriers for these two intrinsic motions are similar to that of enzyme turnover (34 ± 13 kJ/mol), indicating that one or both of these motions are likely involved in the rate-limiting step of catalytic turnover.

of the substrate specificity loop, and perhaps the entire NTD, and disruption of this interaction has been shown to reduce enzymatic activity.[43] Thus, while movement in loop L8 does not configure catalytic amino acids directly, it may coordinate some of the other conformational changes that do.

It is emphasized that the intrinsic motions probed by NMR, while bearing some qualitative similarity, likely do not sample the full extent of substrate-associated conformational changes seen crystallographically. Rigid-domain models fit to NMR residual dipolar coupling (RDC) data show the solution-state average to be closer to the substrate-free crystal structure than to the substrate-bound form.[39] Furthermore, the RDC data show that the subdomains are rotated by different relative amounts. Thus, the likely partially closed state sampled in the intrinsic motions draws from the same repertoire of motions but is mixed together in different proportions.

As described above, previous work has indicated that a conformational change is likely rate-limiting upon the arginine kinase reaction, and more recent work has highlighted the NTD and/or loop L8 motions as candidates.[3,36,38] The similarity between activation energies of these motions and the enzyme-catalyzed reaction provides further support for a model in which a conformational change of one or both of these regions is the rate-limiting step of the enzyme reaction. The activation energy of the arginine kinase reaction is 34 ± 13 kJ/mol, similar to those of other phosphagen kinases: 49 ± 1 and 49 ± 1 kJ/mol for human heart and skeletal muscle creatine kinase, isoform MM, respectively;[44] 45 kJ/mol for shrimp arginine kinase, isoform 2;[37] and 40 kJ/mol for lobster arginine kinase.[38]

It is noted that k_{cat} and k_{ex} are determined at different pH values. Kinetic assays were performed in the standard way to minimize error, at the pH optimum (pH 8).[29,30,45] The NMR is performed where the protein is most stable, pH 6.5. pH−activity profiles indicate that the kinetic activity is 7-fold lower at pH 6.5 and 12 °C.[45] Applying a 7-fold normalization at all temperatures brings k_{cat} values within ±60% of the NMR-determined conformational k_{close} values for the motion of loop L8. A number of caveats apply, particularly that k_{close} is based on a collective fit of

p_B to the dispersion profiles of just the three loop residues whose relaxation exchange can be shown to be in the slow-to-intermediate regime. Considering the many orders over which rates can range, notwithstanding the caveats, the observed order-of-magnitude agreement in the rates of conformational change and enzyme turnover is quite remarkable.

Determination of the activation energies depends on k_{ex} and is not subject to the caveats of p_B fitting. The activation energies for closure of the NTD and loop L8, calculated from k_{ex}, are 46 ± 8 and 34 ± 12 kJ/mol, respectively (Figure 4), while the estimate from k_{close} for L8 is 47 ± 17 kJ/mol. Thus, conformational activation barriers are not only similar to catalytic turnover barriers but also consistent with each other, assuming identical transmission coefficients. Possibilities for the interplay between the NTD and loop L8 motions range from complete independence to a concerted motion in which they are linked. Attempts at fitting a single, two-state concerted-motion model for both regions result in k_{ex} values that are similar to the individually fit models. However, the fitted p_B and $\Delta\omega$ values are quite different. The combined p_B is substantially larger and, in contrast to the separately fit values, shows a marked temperature dependence, ranging from 13.0 to 26.4% over the 15 °C temperature range. Unlike the k_{ex} analysis, this comparison of p_B values is subject to the caveats over the exchange regime already discussed. Thus, the data available are insufficient for a definitive determination of whether the NTD and loop L8 motions are coupled or independent.

As the activation barriers of the enzyme motions were obtained for the substrate-free enzyme, it is tempting to speculate that preformation of an arginine kinase conformation that is amenable to binding substrate is the rate-limiting step.[3] Such a conclusion would be consistent with the enzyme's substrate-associated conformational changes resulting (in part) from conformational selection.[46] Recent analysis of NMR residual dipolar couplings indicates that, in solution, the time-averaged substrate-free arginine kinase has a conformation more like the open-form crystal structure than the closed transition state, but somewhat intermediate.[39] With the full extent of changes seen upon substrate binding, the enzyme wraps around the substrates, occluding the active site, so conformational selection cannot account for all of the changes. It is possible that formation of the encounter complex involves selection among conformations sampled dynamically in the substrate-free state, with additional changes occurring by induced fit.[47] The results here indicate that the rate-limiting step may be the conformational changes involved in selection.

■ ASSOCIATED CONTENT

Supporting Information. Lists of NMR relaxation exchange data (R_2, R_{ex}, and α). This material is available free of charge via the Internet at http://pubs.acs.org.

■ AUTHOR INFORMATION

Corresponding Author

*Department of Biochemistry and Molecular Biology, Oregon Health and Science University, 3181 SW Sam Jackson Park Rd., Portland, OR 97239-3098. E-mail: chapmami@ohsu.edu. Telephone: (503) 494-1025. Fax: (503) 494-8393.

Funding Sources

Supported by the National Institutes of Health (Grant GM77643 to M.S.C.), the National Science Foundation through the National High Magnetic Field Laboratory Institute for Health Research and Policy (Grant DMR-0084173 to J.J.S. and M.S.C.), and the American Heart Association (Grant 0415115B to O.D.).

■ ACKNOWLEDGMENT

We thank W. Ross Ellington and Gregg Hoffman of Florida State University (Tallahassee, FL) for assistance with the steady-state kinetic assay.

■ ABBREVIATIONS

NMR, nuclear magnetic resonance; CPMG, Carr−Purcell−Meiboom−Gill; TROSY, transverse relaxation-optimized spectroscopy; NTD, N-terminal domain; CTD, C-terminal domain; DSS, 4,4-dimethyl-4-silapentane-1-sulfonic acid; NADH/NAD^+, nicotinamide adenine dinucleotide.

■ REFERENCES

(1) Ellington, W. R. (2001) Evolution and Physiological Roles of Phosphagen Systems. *Annu. Rev. Physiol. 63*, 289–325.

(2) Davulcu, O., Clark, S. A., Chapman, M. S., and Skalicky, J. J. (2005) Main chain ^1H, ^{13}C, and ^{15}N resonance assignments of the 42-kDa enzyme arginine kinase. *J. Biomol. NMR 32*, 178.

(3) Davulcu, O., Flynn, P. F., Chapman, M. S., and Skalicky, J. J. (2009) Intrinsic domain and loop dynamics commensurate with catalytic turnover in an induced-fit enzyme. *Structure 17*, 1356–1367.

(4) Yousef, M. S., Clark, S. A., Pruett, P. K., Somasundaram, T., Ellington, W. R., and Chapman, M. S. (2003) Induced fit in guanidino kinases-comparison of substrate-free and transition state analog structures of arginine kinase. *Protein Sci. 12*, 103–111.

(5) Yousef, M. S., Fabiola, F., Gattis, J., Somasundaram, T., and Chapman, M. S. (2002) Refinement of Arginine Kinase Transition State Analogue Complex at 1.2 Å resolution; mechanistic insights. *Acta Crystallogr. D58*, 2009–2017.

(6) Zhou, G., Somasundaram, T., Blanc, E., Parthasarathy, G., Ellington, W. R., and Chapman, M. S. (1998) Transition state structure of arginine kinase: Implications for catalysis of bimolecular reactions. *Proc. Natl. Acad. Sci. U.S.A. 95*, 8449–8454.

(7) Blethen, S. L. (1972) Kinetic Properties of the Arginine Kinase Isoenzymes of *Limulus polyphemus*. *Arch. Biochem. Biophys. 149*, 244–251.

(8) Gattis, J. L., Ruben, E., Fenley, M. O., Ellington, W. R., and Chapman, M. S. (2004) The active site cysteine of arginine kinase: Structural and functional analysis of partially active mutants. *Biochemistry 43*, 8680–8689.

(9) Pruett, P. S., Azzi, A., Clark, S. A., Yousef, M., Gattis, J. L., Somasundaram, T., Ellington, W. R., and Chapman, M. S. (2003) The putative catalytic bases have, at most, an accessory role in the mechanism of arginine kinase. *J. Biol. Chem. 29*, 26952–26957.

(10) Dumas, C., and Janin, J. (1983) Conformational changes in arginine kinase upon ligand binding seen by small-angle X-ray scattering. *FEBS Lett. 153*, 128–130.

(11) Chapman, M. S., and Somasundaram, T. (2010) De-icing: Recovery of diffraction intensities in the presence of ice rings. *Acta Crystallogr. D66*, 741–744.

(12) Fritz-Wolf, K., Schnyder, T., Wallimann, T., and Kabsch, W. (1996) Structure of Mitochondrial Creatine Kinase. *Nature 381*, 341–345.

(13) Lahiri, S. D., Wang, P. F., Babbitt, P. C., McLeish, M. J., Kenyon, G. L., and Allen, K. N. (2002) The 2.1 Å Structure of *Torpedo californica* Creatine Kinase Complexed with the ADP-Mg^{2+}-NO_3^--Creatine Transition-State Analogue Complex. *Biochemistry 41*, 13861–13867.

(14) Ohren, J. F., Kundracik, M. L., Borders, C. L., Jr., Edmiston, P., and Viola, R. E. (2007) Structural asymmetry and intersubunit communication in muscle creatine kinase. *Acta Crystallogr. D63*, 381–389.

(15) Lipari, G., and Szabo, A. (1982) Model-Free approach to the interpretation of Nuclear Magnetic Resonance Relaxation in Macromolecules. 1. Theory and Range of Validity. *J. Am. Chem. Soc. 104*, 4546–4559.

(16) Lipari, G., and Szabo, A. (1982) Model-Free Approach to the Interpretation of Nuclear Magnetic Resonance Relaxation in Macromolecules. 2. Analysis of Experimental Results. *J. Am. Chem. Soc. 104*, 1559–4570.

(17) Cavanagh, J., Fairbrother, W. J., Palmer, A. G., III, and Skelton, A. J. (1996) *Protein NMR Spectroscopy*, Academic Press, San Diego.

(18) Loria, J. P., Rance, M., and Palmer, A. G., III (1999) A TROSY CPMG sequence for characterizing chemical exchange in large proteins. *J. Biomol. NMR 15*, 151–155.

(19) Palmer, A. G., III, Kroenke, C. D., and Loria, J. P. (2001) Nuclear magnetic resonance methods for quantifying microsecond-to-millisecond motions in biological macromolecules. *Methods Enzymol. 339*, 204–238.

(20) Koshland, D. E., Jr. (1958) Application of a theory of enzyme specificity to protein synthesis. *Proc. Natl. Acad. Sci. U.S.A. 44*, 98–104.

(21) Boehr, D. D., Dyson, H. J., and Wright, P. E. (2006) An NMR perspective on enzyme dynamics. *Chem. Rev. 106*, 3055–3079.

(22) Eisenmesser, E. Z., Bosco, D. A., Akke, M., and Kern, D. (2002) Enzyme dynamics during catalysis. *Science 295*, 1520–1523.

(23) Wang, Y., Berlow, R. B., and Loria, J. P. (2009) Role of loop-loop interactions in coordinating motions and enzymatic function in triosephosphate isomerase. *Biochemistry 48*, 4548–4556.

(24) Watt, E. D., Shimada, H., Kovrigin, E. L., and Loria, J. P. (2007) The mechanism of rate-limiting motions in enzyme function. *Proc. Natl. Acad. Sci. U.S.A. 104*, 11981–11986.

(25) Raiford, D. S., Fisk, C. L., and Becker, E. D. (1979) Calibration of methanol and ethylene glycol nuclear magnetic resonance thermometers. *Anal. Chem. 51*, 2050–2051.

(26) Markley, J. L., Bax, A., Arata, Y., Hilbers, C. W., Kaptein, R., Sykes, B. D., Wright, P. E., and Wuthrich, K. (1998) Recommendations for the presentation of NMR structures of proteins and nucleic acids. IUPAC-IUBMB-IUPAB Inter-Union Task Group on the Standardization of Data Bases of Protein and Nucleic Acid Structures Determined by NMR Spectroscopy. *J. Biomol. NMR 12*, 1–23.

(27) Millet, O., Loria, J. P., Kroenke, C. D., Pons, M., and Palmer, A. G. (2000) The Static Magnetic Field Dependence of Chemical Exchange Linebroadening Defines the NMR Chemical Shift Time Scale. *J. Am. Chem. Soc. 122*, 2867–2877.

(28) Schlegel, J., Armstrong, G. S., Redzic, J. S., Zhang, F., and Eisenmesser, E. Z. (2009) Characterizing and controlling the inherent dynamics of cyclophilin-A. *Protein Sci. 18*, 811–824.

(29) Ellington, W. R. (1989) Phosphocreatine represents a thermodynamic and functional improvement over other muscle phophagens. *J. Exp. Biol. 143*, 177–194.

(30) Morrison, J. F., and James, E. (1965) The Mechanism of the Reaction Catalysed by Adenosine Triphosphate-Creatine Phosphotransferase. *Biochem. J. 97*, 37–52.

(31) Segel, I. H. (1975) *Enzyme Kinetics: Behaviour and Analysis of Rapid Equilibrium and Steady-State Enzyme Systems*, Wiley Classics Edition, Wiley, New York.

(32) Segel, I. H. (1975) Cpt IV: Rapid Equilibrium Bireactant and Terreactant Systems. In *Enzyme Kinetics: Behaviour and Analysis of Rapid Equilibrium and Steady-State Enzyme Systems*, Wiley Classics Edition, Wiley, New York.

(33) Mandel, A. M., Akke, M., and Palmer, A. G., III (1996) Dynamics of ribonuclease H: Temperature dependence of motions on multiple time scales. *Biochemistry 35*, 16009–16023.

(34) Baxter, N. J., and Williamson, M. P. (1997) Temperature dependence of ^{1}H chemical shifts in proteins. *J. Biomol. NMR 9*, 359–369.

(35) Beach, H., Cole, R., Gill, M. L., and Loria, J. P. (2005) Conservation of μs—ms enzyme motions in the apo- and substrate-mimicked state. *J. Am. Chem. Soc. 127*, 9167–9176.

(36) Barman, T. E., Travers, F., Bertrand, R., and Roseau, G. (1978) Transient-phase studies on the arginine kinase reaction. *Eur. J. Biochem. 89*, 243–249.

(37) Iwanami, K., Iseno, S., Uda, K., and Suzuki, T. (2009) A novel arginine kinase from the shrimp *Neocaridina denticulata*: The fourth arginine kinase gene lineage. *Gene 437*, 80–87.

(38) Travers, F., Bertrand, R., Roseau, G., and Van Thoai, N. (1978) Cryoenzymologic studies on arginine kinase: Solvent, temperature and pH effects on the overall reaction. *Eur. J. Biochem. 88*, 523–528.

(39) Niu, X., Brüschweiler-Li, L., Davulcu, O., Skalicky, J. J., Brüschweiler, R., and Chapman, M. S. (2011) Arginine Kinase. Joint Crystallographic & NMR RDC Analyses link Substrate-Associated Motions to Intrinsic Flexibility. *J. Mol. Biol. 405*, 479–496.

(40) Jencks, W. P. (1969) *Catalysis in Chemistry and Enzymology*, McGraw-Hill, New York.

(41) Jencks, W. P. (1975) Binding energy, specificity, and enzymic catalysis: the circe effect. *Adv. Enzymol. Relat. Areas Mol. Biol. 43*, 219–410.

(42) Jencks, W. P., and Mage, M. I. (1974) "Orbital Steering", Entropy and Rate Accelerations. *Biochem. Biophys. Res. Commun. 57*, 887–892.

(43) Suzuki, T., Kawasaki, Y., Furukohri, T., and Ellington, W. R. (1997) Evolution of phosphagen kinase. VI. Isolation, characterization and cDNA-derived amino acid sequence of lombricine kinase from the earthworm *Eisenia foetida*, and identification of a possible candidate for the guanidine substrate recognition site. *Biochim. Biophys. Acta 1343*, 152–159.

(44) Hagelauer, U., and Faust, U. (1982) The catalytic activity and activation energy of creatine kinase isoenzymes. *J. Clin. Chem. Clin. Biochem. 20*, 633–638.

(45) Rao, B. D., and Cohn, M. (1977) ^{31}P nuclear magnetic resonance of bound substrates of arginine kinase reaction: Chemical shifts in binary, ternary, quaternary, and transition state analog complexes. *J. Biol. Chem. 252*, 3344–3350.

(46) Ma, B., Kumar, S., Tsai, C. J., and Nussinov, R. (1999) Folding funnels and binding mechanisms. *Protein Eng. 12*, 713–720.

(47) Bakan, A., and Bahar, I. (2009) The intrinsic dynamics of enzymes plays a dominant role in determining the structural changes induced upon inhibitor binding. *Proc. Natl. Acad. Sci. U.S.A. 106*, 14349–14354.